



## RESEARCH ARTICLE

# Characterization of polyphosphate dynamics in the widespread freshwater diatom *Achnantheidium minutissimum* under varying phosphorus supplies

Adrien Lapointe<sup>1</sup>  | Mustafa Kocademir<sup>2</sup> | Paavo Bergman<sup>3</sup>  | Imaiyan Chitra Ragupathy<sup>4</sup> | Michael Laumann<sup>3</sup> | Graham J. C. Underwood<sup>5</sup> | Andreas Zumbusch<sup>2</sup> | Dieter Spiteller<sup>1</sup> | Peter G. Kroth<sup>1</sup>

<sup>1</sup>Department of Biology, University of Konstanz, Konstanz, Germany

<sup>2</sup>Department of Chemistry, University of Konstanz, Konstanz, Germany

<sup>3</sup>Electron-Microscopy Centre, University of Konstanz, Konstanz, Germany

<sup>4</sup>Department of Clinical Medicine, Aarhus University, Aarhus, Denmark

<sup>5</sup>School of Life Sciences, University of Essex, Colchester, UK

## Correspondence

Adrien Lapointe, Department of Biology, University of Konstanz, Konstanz, Germany.

Email: [adrien.lapointe31@gmail.com](mailto:adrien.lapointe31@gmail.com)

## Funding information

Deutsche Forschungsgemeinschaft, Grant/Award Number: GRK2272 (RTG R3)

Editor: R. Wetherbee

## Abstract

Polyphosphates (polyP) are ubiquitous biomolecules that play a multitude of physiological roles in many cells. We have studied the presence and role of polyP in a unicellular alga, the freshwater diatom *Achnantheidium minutissimum*. This diatom stores up to 2.0 pg·cell<sup>-1</sup> of polyP, with chain lengths ranging from 130 to 500 inorganic phosphate units (P<sub>i</sub>). We applied energy dispersive X-ray spectroscopy, Raman/fluorescence microscopy, and biochemical assays to localize and characterize the intracellular polyP granules that were present in large apical vacuoles. We investigated the fate of polyP in axenic *A. minutissimum* cells grown under phosphorus (P), replete (P<sub>(+)</sub>), or P deplete (P<sub>(-)</sub>) cultivation conditions and observed that in the absence of exogenous P, *A. minutissimum* rapidly utilizes their internal polyP reserves, maintaining their intrinsic growth rates for up to 8 days. PolyP-depleted *A. minutissimum* cells rapidly took up exogenous P a few hours after P<sub>i</sub> resupply and generated polyP three times faster than cells that were not initially subjected to P limitation. Accordingly, we propose that *A. minutissimum* deploys a succession of acclimation strategies regarding polyP dynamics where the production or consumption of polyP plays a central role in the homeostasis of the diatom.

## KEYWORDS

*Achnantheidium minutissimum*, diatom, electron microscopy, phosphate uptake, polyphosphate, stimulated Raman scattering microscopy

## INTRODUCTION

Phosphorus (P) is an essential element playing an important role in all living organisms (Paytan & McLaughlin, 2007). Phosphorus in the form of phosphate (P<sub>i</sub>) is incorporated into vital biomolecules such as nucleic acids and, therefore, is crucial for the storage,

replication, and transcription of genetic information. In addition, P<sub>i</sub> is critical for the effective production of ATP for intracellular energy storage and for structural components such as phospholipids for membrane formation. If P availability becomes limited, primary production in the ocean (Benitez-Nelson, 2000) and lake ecosystems (Li et al., 2019) can be strongly affected.

**Abbreviations:** AM, *Achnantheidium* medium; BM, Bacillariophycean medium; ddH<sub>2</sub>O, double distilled water; EDX, energy-dispersive X-ray; H<sub>2</sub>SO<sub>4</sub>, sulfuric acid; K<sub>2</sub>HPO<sub>4</sub>, dipotassium hydrogen phosphate; P, phosphorus; P<sub>(-)</sub>, phosphate-deplete; P<sub>(-/+)</sub>, phosphate-deplete subsequently followed by phosphate-replete; P<sub>(+)</sub>, phosphate-replete; P<sub>(+/+)</sub>, phosphate-replete subsequently followed by phosphate-replete; P<sub>i</sub>, inorganic phosphate; polyP, polyphosphate; SEM, scanning electron microscopy; SRS, stimulated Raman scattering.

This is an open access article under the terms of the [Creative Commons Attribution-NonCommercial-NoDerivs](https://creativecommons.org/licenses/by-nc-nd/4.0/) License, which permits use and distribution in any medium, provided the original work is properly cited, the use is non-commercial and no modifications or adaptations are made.

© 2024 The Authors. *Journal of Phycology* published by Wiley Periodicals LLC on behalf of Phycological Society of America.

It is known that microalgae have developed adaptive responses to cope with low ambient P, including enzymatic use of extracellular dissolved organic P, a decrease in cellular P demands, and cellular P storage (Lin et al., 2016). The benthic diatom *Seminavis robusta* actively moves towards P sources (Bondoc et al., 2019). Under high-P conditions, microalgae can store excess  $P_i$  intracellularly by the formation of inorganic polyphosphates (polyP) and use it to alleviate future P limitation (Sanz-Luque et al., 2020). These are linear polymers composed of inorganic phosphate units linked by energy-rich phosphoanhydride bonds comprising from three up to several thousand phosphate monomers. PolyP exists ubiquitously in all kingdoms of life (Brown & Kornberg, 2004; Docampo et al., 2005; Sanz-Luque et al., 2020). Displaying a granular shape, polyP was initially called “metachromatic granules” (Babes, 1895) or “volutin granules” (Meyer, 1904) and later renamed polyP granules (Wiame, 1947). This inorganic polymer was first isolated from yeast (Lieberman, 1890) and much later from microalgae (Fisher, 1971). PolyP fulfills a large number of functions (Rao et al., 2009; Xie & Jakob, 2019): In bacteria, polyP is involved in stress resistance, biofilm formation, quorum-sensing, and virulence (Rao et al., 1998; Rashid et al., 2000). In *Saccharomyces cerevisiae*, polyP was observed to chelate metal ions, preventing metal ion-induced cellular damage (Trilisenko et al., 2017) and to be important for yeast cell survival upon DNA damage (Bru et al., 2017) and for the accumulation and metabolism of  $P_i$  in yeast (Ogawa et al., 2000).

Although the function of polyP in microalgae under P limitation has attracted attention in recent years (Li & Dittrich, 2019; Plouviez et al., 2021; Solovchenko et al., 2020), only a handful of studies have focused on polyP production in diatoms. Diatoms constitute one of the most diverse and ecologically important groups of eukaryotic phytoplankton. They exist in all aquatic systems, and they are responsible for about one-fifth of global photosynthesis (Armbrust, 2009). PolyP production by diatoms plays a key role in the sequestration of P within the marine sediment and contributes to the formation of calcium–phosphate apatite (Diaz et al., 2008). However, studies focusing on polyP occurrence and production in diatoms are scarce. In *Phaeodactylum tricorutum*, polyP amounts and sizes have been described as a function of osmotic conditions (Leitão et al., 1995). Volutin granules were observed in raphid (Mann, 1985), as well as in centric diatoms (Bedoshvili et al., 2018). Taking into account nutrient variations, a few studies have focused on the regulatory mechanisms that link changes in the environmental phosphate concentrations to polyP synthesis in diatoms (Dyhrman et al., 2012). Therefore, to understand the mechanisms of polyP dynamics in diatoms, more systematic studies detecting and monitoring polyP dynamics under different P availabilities are required.

In this study, we therefore investigated the role of polyP in the freshwater diatom *Achnantheidium minutissimum*, a species that is observed widely not only in alkaline and acidic but also in oligotrophic and hypertrophic environments (Hlúbiková et al., 2011; Potapova & Hamilton, 2007; Round, 2004). Because of its ubiquity in different aquatic habitats, *A. minutissimum* serves as an excellent model for shedding light on the effects of P availability on polyP accumulation in freshwater diatoms. We hypothesized that *A. minutissimum* builds up polyP stocks under high P availability to overcome later P-limitation. To test this hypothesis, we cultured *A. minutissimum* in either P-rich or P-limited conditions over 10 days and subsequently resupplied the cells with a P-rich medium. We monitored cell growth, phosphate uptake, and polyP detection within cells at the different growth stages.

## MATERIALS AND METHODS

### Growth conditions and experimental cultures

The freshwater diatom *Achnantheidium minutissimum* (strain MW1) was isolated from photoautotrophic, epilithic biofilms in Lake Constance, Germany (47°41' N; 9°11' E). The associated bacteria were removed using the antibiotic imipenem (Windler et al., 2012). Cultures of axenic diatoms were cultivated at standard conditions at 20°C, under a 16:8 light:dark cycle with a light intensity of  $70 \mu\text{mol photons}\cdot\text{m}^{-2}\cdot\text{s}^{-1}$  and with constant shaking at 130 rpm. Diatoms were cultivated in *Achnantheidium* medium (AM; Windler, 2014), a modified, basal version of Bacillariophycean medium (BM; Schlösser, 1994) lacking soil extract. Vitamins, silica, selenate, and trace metal ions solution were supplemented as described for the F/2 medium (Guillard, 1975). For the study, two different inorganic phosphate ( $P_i$ ;  $K_2HPO_4$ ) treatments within AM were compared with  $\sim 53 \mu\text{M } P_i$ , accounting for P-replete ( $P_{(+)}$ ), and no addition of  $K_2HPO_4$ , accounting for P-deplete ( $P_{(-)}$ ), conditions. Cells were cultivated in glassware, which was washed once beforehand with 0.1 M HCl and thrice with double distilled water ( $\text{ddH}_2\text{O}$ ).

A stock culture of axenic *Achnantheidium minutissimum* (5L) was grown in AM  $P_{(+)}$  under the standard conditions described above; half of the culture was discarded weekly and replaced by the same volume of new AM  $P_{(+)}$ . This semi-batch culture approach maintained the stock culture cells in exponential phase growth, with cell densities between  $\sim 400,000$  and  $1.0 \times 10^6$  cells·mL<sup>-1</sup>. Before starting experiments, 55 mL of the stock culture was sampled and split into the following subsamples: 25 mL for polyP size distribution, 25 mL for scanning electron microscopy (SEM) analyses, 500  $\mu\text{L}$  for vacuolar membrane visualization, and

1 mL for stimulated Raman scattering (SRS; description of the procedures below). The rest of the stock culture was left overnight under the same standard conditions described above, but without shaking to allow cell sedimentation. Consecutively to the overnight sedimentation, the supernatant was discarded and cells were resuspended with 200 mL of new AM P<sub>(+)</sub>. Cells were resuspended by gentle shaking and split into two equal volumes of 100 mL and centrifuged (5000 g, 5 min). The supernatant was discarded and cell pellets were resuspended carefully with 400 mL of either new AM P<sub>(+)</sub> or AM P<sub>(-)</sub>. Subsequently, 100 mL of each of four P<sub>(+)</sub> samples were transferred to four 3.0-L flasks (VWR, Borosilicate Erlenmeyer, Germany) each containing 1900 mL of AM P<sub>(+)</sub>, and 100 mL of each four P<sub>(-)</sub> samples were transferred to four 3.0-L borosilicate flasks each containing 1900 mL of AM P<sub>(-)</sub>. Starting cell concentrations in each culture were about  $130 \times 10^3$  cells·mL<sup>-1</sup>. Cells were cultivated for 15 days as described above. Aliquots were taken 0, 2, 4, 6, 8, 10, 12, and 15 days after inoculation. After sampling on day 15, 420 mL and 240 mL of P<sub>(+)</sub> and P<sub>(-)</sub> cultures, respectively, were discarded, and the remaining cells were supplemented with new AM P<sub>(+)</sub> up to a volume of 2 L to reach a similar cell concentration of  $\sim 200,000$  cells·mL<sup>-1</sup> in both treatments. Additional aliquots were taken after the resupply on day 15 as well as on days 16, 17, and 18. Each aliquot consisted of 160 mL of sample and was subjected to the same procedures for measuring the parameters as described below, except for the aliquots taken on day 15 after the resupply with AM P<sub>(+)</sub> that consisted of only 1 mL used for measuring the cell number and the exogenous P concentration in the cultures.

## Screening for bacterial contaminations

On days 0, 10, and 18, small aliquots (500  $\mu$ L) were taken from the cultures and screened for bacterial contamination using the fluorescent nucleic acid staining SYBR Green I (Cambrex, Rockland, ME USA; Windler et al., 2012). During the experiments, no bacterial contamination was observed.

## Cell counts and growth rate

To quantify cell density, 100  $\mu$ L of resuspended cells were taken from the original aliquots, and cells were counted using a Coulter-counter (Beckman, Multisizer 4 Coulter cell counter®, Germany). The growth rate was estimated from cell concentration measurements during the exponential phase using the following equation (Levasseur et al., 1993):

$$\mu (\text{d}^{-1}) = \frac{\ln(C_x \div C_{x-n})}{t_x - t_{x-n}},$$

where  $\mu$  is the growth rate,  $C$  is cell concentration (cells·mL<sup>-1</sup>),  $t$  is time (day),  $x$  is the harvesting day point, and  $x-n$  is the preceding harvesting day point. For example, for calculating the growth rate occurring between days 2 and 4,  $t_x$  was 4 and  $t_{x-n}$  was 2.

## Quantification of dissolved extracellular phosphate

Following the cell counts, original aliquots were centrifuged (5000 g, 5 min), and 1 mL of the supernatant was taken for analysis of dissolved orthophosphate (P<sub>i</sub>) concentration using a colorimetric assay. The analysis was carried out in a 96 well-plate using the ascorbate-antimony-molybdate assay described by Christ and Blank (2018). In total, 150  $\mu$ L of each sample were pipetted into one well of a 96 microplate. Elsewhere in the microplate, 150  $\mu$ L of the phosphate standard K<sub>2</sub>HPO<sub>4</sub> (0–100  $\mu$ M P<sub>i</sub>) were added in triplicate. Then, 50  $\mu$ L of the phosphate detection reagent containing ammonium heptamolybdate (2.4 mM), H<sub>2</sub>SO<sub>4</sub> (600 mM), antimony potassium tartrate (0.6 mM), and ascorbic acid (88 mM) were added to the wells. After 2 min of incubation at room temperature and gentle mixing, the absorbance of the samples was determined at 882 nm. The lowest amount of P<sub>i</sub> that could be determined with suitable precision and accuracy was given by the limit of quantitation (LOQ, ca. 3  $\mu$ M P<sub>i</sub>; ICH Guideline, 1996; see also equation 1 in Lapointe et al., 2022).

## PolyP quantification

The rest of the supernatant of the centrifuged original aliquots was discarded, and cells were resuspended in either 1 mL of ddH<sub>2</sub>O or 2 mL (when samples were needed for stimulated Raman scattering, SRS, microscopy). In the latter case, the resuspended cell volume was pipetted into two tubes of 1 mL each. Subsequently, the first tube containing the sample for polyP quantification was centrifuged (5000 g, 5 min) and the supernatant was discarded. The second tube was subjected to SRS microscopy. Cell pellets generated for polyP analyses were frozen in liquid N<sub>2</sub> and kept at  $-80^\circ\text{C}$ . PolyP was extracted, purified, and quantified following the protocol described in Lapointe et al. (2022). Extraction and purification were performed using a DNA isolation kit based on cell lysis and gel filtration. For quantification, the purified polyP within the samples was specifically hydrolyzed to P<sub>i</sub> by the recombinant *Escherichia coli* exopolyphosphatase (PPX, MyBiosource, Inc., San Diego, California, USA) in a 96-well plate, following the protocol developed by Christ and Blank (2018) with modifications (Lapointe et al., 2022). In total, 100  $\mu$ L of a diluted polyP extract were pipetted into two different wells of a 96-well plate. One well was supplemented with 50  $\mu$ L of enzyme

reaction buffer (magnesium acetate 15 mM, Tris 60 mM, ammonium acetate 150 mM, pH 7.7). The other well was supplemented with 49  $\mu\text{L}$  of enzyme reaction buffer and 1  $\mu\text{L}$  PPX (1  $\text{mg}\cdot\text{mL}^{-1}$ ). Dipotassium hydrogen phosphate ( $\text{K}_2\text{HPO}_4$ ) standards were pipetted elsewhere on the microplate (see quantification of dissolved extracellular phosphate section). After 1 h of incubation at 37°C in a plate reader (Infinite® 200 PRO, TECAN),  $\text{P}_i$  concentrations were measured using the ascorbate-antimony-molybdate assay described above (see quantification of dissolved extracellular phosphate section), and the polyP content in each well was calculated using equation 2 in Lapointe et al. (2022). The LOQ was measured as described above.

### Size distribution of polyP from *Achnanthydium minutissimum*

PolyP was extracted and purified from the stock culture sample containing 25 mL of *Achnanthydium minutissimum* cells cultivated in AM  $\text{P}_{(+)}$  using the protocol described above. The purified extract was split into two subsamples of equal volume. In a 96-well plate, 100  $\mu\text{L}$  of each subsample was transferred into two wells and subjected to polyP quantification, with the exception that the phosphate detection reagent was added for only one subsample. This procedure allowed the determination of the polyP concentration in the starting culture sample (~5 nmol), and the production of an extracted and purified polyP sample for PPX treatment and control. PolyP was separated on a 20% acrylamide TBE-urea gel (5.8 M urea; 10 mL 30% acrylamide/bisacrylamide, 19:1; 3 mL 5  $\times$  TBE; 1.8 mL  $\text{ddH}_2\text{O}$ ; 150  $\mu\text{L}$  10% ammoniumperoxosulfate; 15  $\mu\text{L}$  TEMED). Five  $\mu\text{L}$  of the polyP standards (405 pmol P) containing average chain-length polyP of 14, 60, 130 (polyP-14, -60, -130, RegeneTiss Incorporated, Nagano, Japan), and 700 (polyP-700, Kerofast, Boston, USA)  $\text{P}_i$  units, as well as 5  $\mu\text{L}$  of the extracted and purified polyP sample with and without PPX treatment were mixed with 5  $\mu\text{L}$  of 2  $\times$  loading dye (2  $\times$  TBE, 6% Ficoll 400, 0.04 bromophenol blue) and loaded on the acrylamide gel. Finally, 10  $\mu\text{L}$  of 10bp (O'RangeRuler 10bp DNA Ladder, ThermoScientific, Germany) and 100bp DNA ladders (Invitrogen, Germany) were loaded as size references. The gel was run at 150 V for about 45 min at room temperature. PolyP was visualized by negative DAPI staining (Smith & Morrissey, 2007). The size range of polyP chain length was estimated by comparing DNA ladder bands and polyP standards as described in Smith et al. (2018).

### Scanning electron microscopy

The second sample from the stock culture containing 25 mL of *Achnanthydium minutissimum* cells

cultivated in AM  $\text{P}_{(+)}$  was centrifuged (5000 g, 5 min). The cell pellets were packed by capillarity into cellulose capillaries (200  $\mu\text{m}$  diameter, Leica microsystems). Within a petri dish containing ~5 mL of AM  $\text{P}_{(+)}$ , the capillaries were cut carefully using a scalpel for sealing each side. Capillaries were sequentially transferred to fixing buffer and subsequently dehydrated using ~1 mL of increasing ethanol concentrations, followed by an additional dehydration using ~1 mL of an acetone gradient. Cells were embedded in an increasing gradient of modified SPURR resin dissolved in absolute acetone. SPURR was prepared using the catalyst DMAE (Ted Pella, INC., Redding, California, USA), NSA (Serva, Heidelberg, Germany) and ERL 4221 (EMS, Hatfield, Pennsylvania, USA). After the acetone completely evaporated, capillaries were transferred to silicone molds that were filled with fresh resin mixture and left for polymerization for 2 day at 65°C. A detailed fixation protocol is found in Table S1 in the Supporting Information. The samples were sectioned using a diamond knife (Diatome, Biehl, Switzerland). The resulting 500-nm sections were placed upon droplets of  $\text{ddH}_2\text{O}$  water on indium tin oxide-coated coverslips. Samples were sputtered with carbon (C) to a thickness of 10 nm (Balzers SCD030; Oerlikon Balzers, Balzers, Liechtenstein). Sections were analyzed by energy-dispersive X-ray spectroscopy (SEM-EDX) in a Zeiss Auriga FESEM (Zeiss, Oberkochen, Germany) equipped with an X-Max 20  $\text{mm}^2$  detector (Oxford Instruments, Abingdon, UK).

### Stimulated Raman microscopy of *Achnanthydium minutissimum*

To visualize polyP granules in *Achnanthydium minutissimum*, the cells were imaged using SRS microscopy (Cheng & Xie, 2015). Measurements for SRS of *A. minutissimum* were carried out using a Leica SP8 microscope with SRS capability (Leica Microsystems, Mannheim, Germany). For the analysis, the 1 mL stock culture sample (see cell concentration and growth rate section) as well as the 1 mL experiment aliquots (see polyP quantification section) were processed as follows. Each sample was centrifuged (5000 g, 1 min), and the supernatant was discarded. The cell pellet was resuspended with 40  $\mu\text{L}$  of 1% w/v of a low-gelling agarose solution (Sigma Aldrich, Taufkirchen, Germany) to prevent the movement of cells during analysis (Moudrikova et al., 2017). A small drop (10  $\mu\text{L}$ ) of the sample was pipetted between two glass coverslips (24  $\times$  60 mm, Menzel-Gläser, Heidelberg, Germany) and sealed with an imaging spacer (SecureSeal, Sigma Aldrich, Taufkirchen, Germany). Before analysis, samples were subjected to photobleaching of the carotenoids. Regions containing diatoms were subjected to the maximum

power of the microscope's 488 nm laser for 15–20 min. PolyP granules were detected by SRS imaging at  $1166\text{ cm}^{-1}$ . If necessary, several frames were made from each sample in different areas of the bleached sample to obtain data from at least 100 cells. A Python script was used to automatically determine the percentage of cells containing at least one visible granule on the SRS pictures based on the bright pixels. These data were used to calculate the relative area covered by the polyP granules within each cell containing granules. Spontaneous Raman spectra were recorded using a commercial Raman microscope (MonoVista CRS, S&I, Warstein, Germany) with excitation at 488 nm.

## Vacuoles staining in *Achnantheidium minutissimum*

For visualization of vacuolar structures in *Achnantheidium minutissimum*, we used the fluorescent membrane marker MDY-64 (Molecular probes, Leiden, Netherlands), following the protocol of Huang et al. (2016) with modifications. Cells were incubated in  $2\text{ }\mu\text{M}$  MDY-64 in the dark for 2 min at room temperature, and fluorescence was analyzed using an epifluorescence microscope Olympus BX51 (Olympus Europe, Hamburg, Germany) equipped with a Zeiss AxioCam MRm digital camera system (Carl Zeiss MicroImaging GmbH, Göttingen, Germany).

## Data analysis

GraphPad Prism 9.1.2 was used to conduct all statistical analyses. All data were checked for normality and homoscedasticity. We used *t*-tests for comparing two groups of data and the analysis of variance (ANOVA) when more than two groups of data were compared. A dataset combining mean values of growth rate, external P concentration, polyP concentration, and P uptake was made for each  $P_{(-)}$  and  $P_{(+)}$  treatment, before and after resupply with P. We generated a Spearman's rank correlation coefficient for each datasets separately, as well as for the combined  $P_{(+)}$  and  $P_{(-)}$  dataset, to assess significant relationships between the above-mentioned variables.

## RESULTS

### *Achnantheidium minutissimum* possesses polyP-containing granules enclosed in vacuoles

To study the presence of polyP granules in diatoms, we performed scanning electron microscopy (SEM) of a section containing *Achnantheidium minutissimum* cells cultivated in P-replete ( $P_{(+)}$ ) conditions and observed spherical structures (Figure 1a, green arrowhead).

These granules appeared to be filled with electron-dense material and localized in the two apices of the diatom. Granules were enclosed in an uncharacterized area differing from the rest of the cellular components by poor electron density (Figure 1a, blue arrowhead). Using the same SEM sample, we employed energy-dispersive X-ray analyses (EDX) to investigate the molecular composition of the granules and detected an increased amount of phosphorus (P) and calcium (Ca) in the granules (Figure 1b) when compared to other areas of the cell (Figure 1c). Both P and Ca appeared to be distributed homogeneously within the granules, and the P peak was much stronger than the Ca peak (Figure 1b,c; Figures S1B,C in the Supporting Information), indicating that the granules contained higher amounts of P than Ca. The locations of the granules within the *A. minutissimum* cells was investigated by epifluorescence microscopy using MDY-64, which specifically stains vacuolar membranes (Figure 2). Most of *A. minutissimum* cells in the sample contained one or two large vacuoles (Figure 2). The two apical vacuoles were located in the same cellular area as the P-containing granules observed by SEM and EDX (Figure 2b), one on each apex of the cell and in close contact with large circular structures (Figure 2a), confirmed as lipid droplet by BODIPY staining (Figure S2 in the Supporting Information).

We furthermore investigated the molecular state of the P moieties detected in the granules using stimulated Raman scattering (SRS) based microscopy (Figure 3), allowing the specific imaging of polyP, represented by a strong peak in the area of  $1145\text{--}1177\text{ cm}^{-1}$  (De Jager & Heyns, 1998; Fernando et al., 2019). The SRS spectra of polyP and lipids of *Achnantheidium minutissimum* cells cultivated in  $P_{(+)}$  conditions are shown and compared to spontaneous Raman spectra of the polyP and fatty acid standards (hexametaphosphate and oleic acid) in Figure 3b,c, respectively. The granules (Figure 3a, green pixels) revealed an intense peak at  $1166\text{ cm}^{-1}$  (Figure 3b), representing polyP.

### Estimation of polyP chain-lengths from *Achnantheidium minutissimum*

To determine the lengths of the polyP chains in *Achnantheidium minutissimum*, polyP from cells cultivated in  $P_{(+)}$  condition was isolated and purified using an optimized size exclusion method (Lapointe et al., 2022) and subjected to acrylamide TBE-urea electrophoresis. The polyP sample was compared to defined polyP standards and DNA size markers (Smith et al., 2018; Figure 4). The polyP standards consist of heterogeneous mixtures of chain lengths resulting in a smear instead of a single band. The polyP fraction of *A. minutissimum* comprised polyP chain lengths of  $130\text{--}500 P_i$  units (Figure 4). Treating the samples with PPX, which cleaves polyP from the terminal ends and

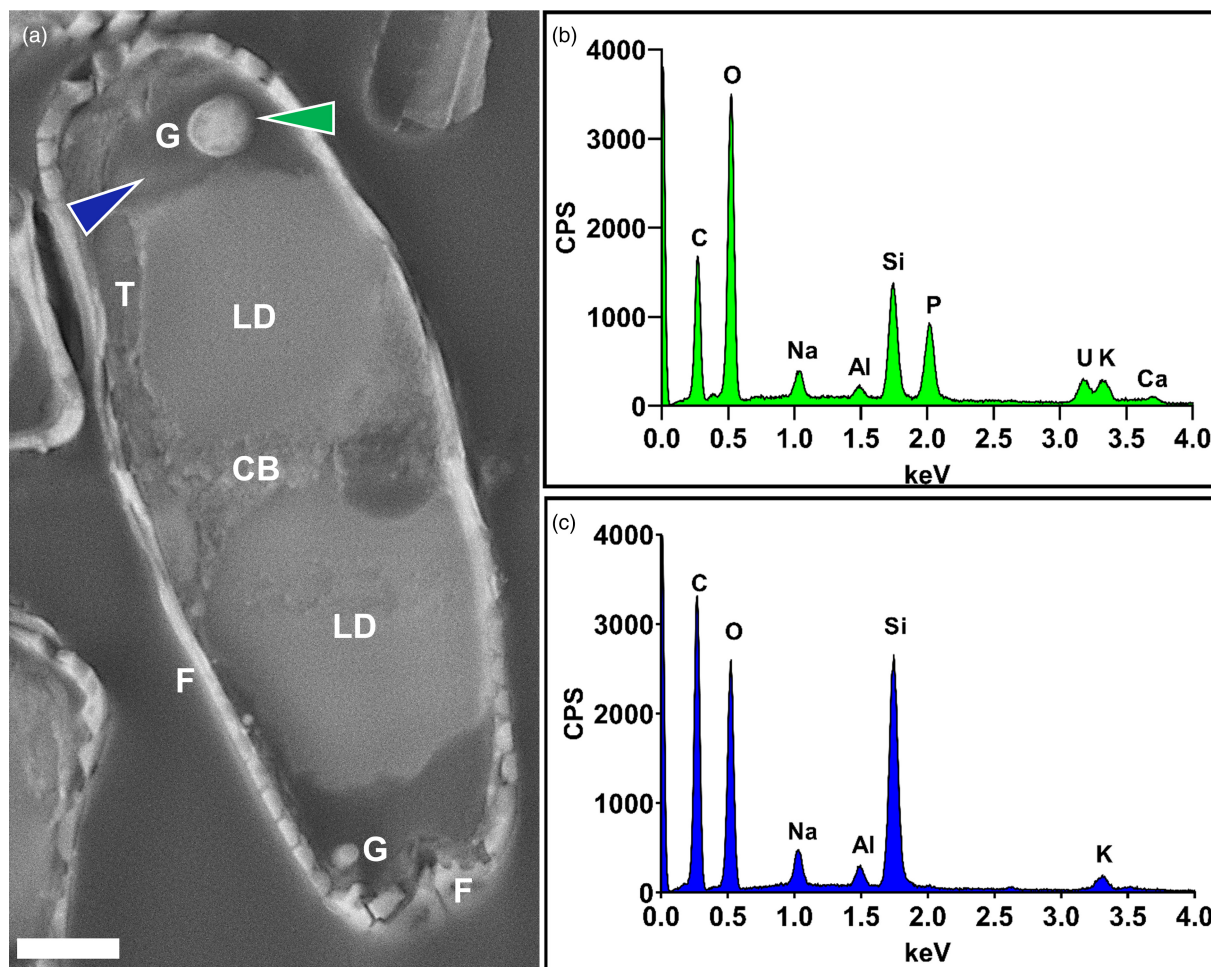


**FIGURE 1** Detection of granules containing phosphorus in an *Achnantheidium minutissimum* cell. (a) Ultrastructural sectional SEM image of *A. minutissimum* containing a cytoplasmic bridge (CB), thylakoids (T), lipid droplets (LD), electron-dense granule (G), and (F) frustule. (b) EDX spectrum of the electron-dense granule (recorded from the area indicated by the green arrowhead). The peaks at 2.01 and 3.69 keV indicate phosphorus (P) and calcium (Ca), respectively. (c) EDX spectrum of a cellular area with no granule (recorded from the area indicated by the blue arrowhead) showing the absence of P and Ca peaks. These data are representative of cells cultivated in P-replete ( $P_{(+)}$ ) conditions. The scale bar (white) represents 1  $\mu\text{m}$ . [Color figure can be viewed at [wileyonlinelibrary.com](http://wileyonlinelibrary.com)]

releases a  $P_i$ , resulted in complete degradation of the polyP fraction, confirming its identity.

### Impact of phosphate availability on diatom physiology

To study responses to different phosphate ( $P_i$ ) availabilities, we cultured *Achnantheidium minutissimum* under P replete ( $P_{(+)}$ ) and deplete ( $P_{(-)}$ ) conditions. The lag phase of cells grown in  $P_{(+)}$  and in  $P_{(-)}$  conditions both occurred within 2 days and was followed by an exponential growth phase from day 2 to day 10 (Figure 5a). In both conditions, the cells entered the stationary phase on day 10 (Figure 5a). The final cell density on day 15 was 2.3 times higher for *A. minutissimum* cultivated in  $P_{(+)}$  compared to cells in  $P_{(-)}$  conditions before resupplying in AM  $P_{(+)}$ . Cells cultivated in  $P_{(-)}$  conditions grew for 8 days even though there was no exogenous P detectable (Figure 5a). Only between days 4 to 6 did the

growth rates of cells grown in  $P_{(-)}$  and  $P_{(+)}$  conditions differ significantly (Student test:  $t(6)=3.799$ ,  $p=0.090$ ; Table S2 in the Supporting Information). After a 5-day stationary phase, cultures were resupplied with  $P_{(+)}$  cultivation medium on day 15. Cells having experienced either  $P_{(+)}$  or  $P_{(-)}$  conditions (referred to as  $P_{(+/-)}$  cells and  $P_{(-/+)}$  cells) both simultaneously resumed growth after a lag phase of about 24 h, and cultures started to divide again at day 17 (Figure 5a).  $P_{(-/+)}$  and  $P_{(+/-)}$  cells yielded slightly but significantly lower final cell numbers for  $P_{(-/+)}$  cells with  $2.41 \times 10^6 \pm 0.19 \times 10^6$  cell·mL<sup>-1</sup> than for  $P_{(+/-)}$  cells with  $3.02 \times 10^6 \pm 0.23 \times 10^6$  cell·mL<sup>-1</sup>, respectively (Table S3 in the Supporting Information). The extracellular  $P_i$  concentrations in  $P_{(+)}$  cultures started from  $53.3 \pm 0.77$   $\mu\text{M}$   $P_i$  at day 0 in  $P_{(+)}$  cultivation medium (Figure 5b).  $P_{(+)}$  cells started to take up  $P_i$  during the lag phase with rates of  $3.93 \pm 1.21$  pg  $P_i$ ·cell<sup>-1</sup>·day<sup>-1</sup> from day 0 to day 2 (Figure 5d). During cell division, levels of  $P_i$  uptake per cell were about five times lower than during the lag phase with  $0.67 \pm 0.19$  pg  $P_i$ ·cell<sup>-1</sup>·day<sup>-1</sup> and

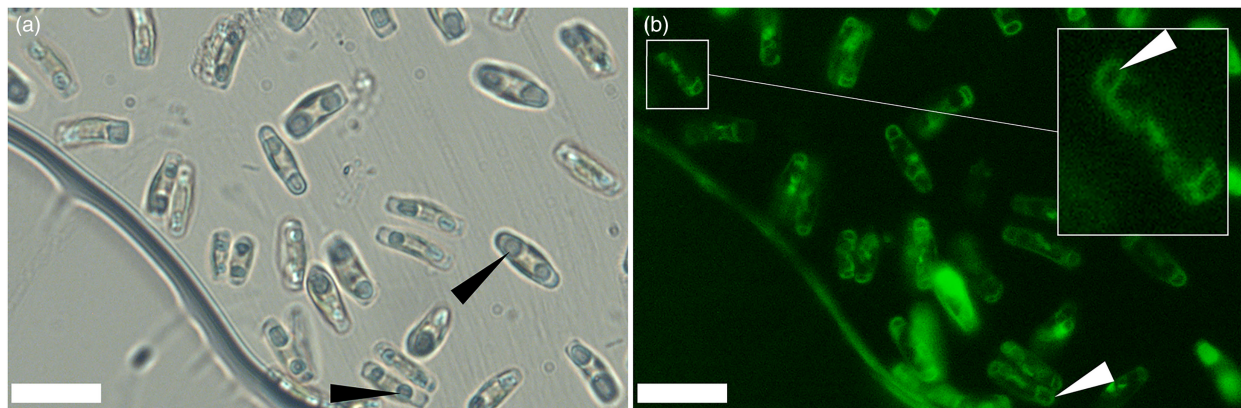


**FIGURE 2** Localization of the vacuoles in the diatom *Achnantheidum minutissimum*. (a) Bright-field micrograph of *A. minutissimum* cells containing lipid droplets (black arrowheads). (b) Epifluorescence of a marker for vacuole membrane (MDY-64) indicates the location of the vacuoles (white arrowheads). These data are representative of cells cultivated in P-replete ( $P_{(+)}$ ) conditions. Scale bars represent 10  $\mu\text{m}$ . [Color figure can be viewed at [wileyonlinelibrary.com](https://onlinelibrary.wiley.com/doi/10.1111/jpy.13423)]

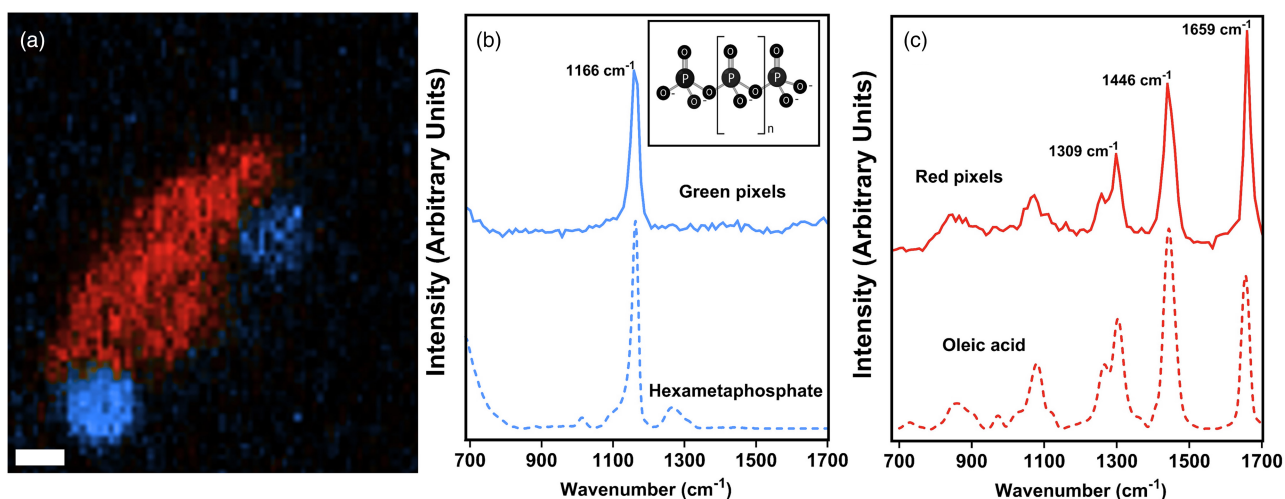


**FIGURE 3** PolyP detection in *Achnantheidum minutissimum* cells using stimulated Raman scattering (SRS) microscopy. (a) SRS map of *A. minutissimum* cells showing the distribution of polyP (blue pixels) and lipids (red pixels; scale bar: 1  $\mu\text{m}$ ). (b) Spontaneous Raman spectrum of a polyP standard of sodium hexametaphosphate of 96% purity (Sigma Aldrich, Taufkirchen, Germany; green dotted line), and SRS spectrum of intracellular granules (solid blue line), showing a maximum at 1166  $\text{cm}^{-1}$ . A structure of linear polyP is shown in the upper right ( $n = 1$  to several 100 of  $P_i$ ). (c) Spontaneous Raman spectrum of oleic acid as a lipid standard (oleic acid, red dotted line) and SRS spectrum of the lipid distribution within the diatom (solid red line), showing three major maxima at 1309, 1446, and 1659  $\text{cm}^{-1}$ . These data are representative of polyP-rich cells cultivated in P-replete ( $P_{(+)}$ ) conditions. [Color figure can be viewed at [wileyonlinelibrary.com](https://onlinelibrary.wiley.com/doi/10.1111/jpy.13423)]

$0.57 \pm 0.04 \text{ pg } P_i \cdot \text{cell}^{-1} \cdot \text{day}^{-1}$  from days 2 to 4 and days 4 to 6, respectively (Figure 5d). At day 6, levels of exogenous P in  $P_{(+)}$  cultures were below the limit of quantification (LOQ,  $<3 \mu\text{M } P_i$ ; Figure 5b). In  $P_{(-)}$  cultures, there were no detectable amounts of exogenous  $P_i$  from day 0 to day 15 (Figure 5b). During the first 48 h of the lag phase, polyP amounts in  $P_{(+)}$  cells increased at a rate of  $0.14 \pm 0.09 \text{ pg } P_i \cdot \text{cell}^{-1} \cdot \text{day}^{-1}$ , further increasing during cell division to  $0.32 \pm 0.08 \text{ pg } P_i \cdot \text{cell}^{-1} \cdot \text{day}^{-1}$  until day 4 (Figure 5c, Table S4 in the Supporting Information). On day 6, when exogenous  $P_i$  levels were no longer detectable, polyP concentrations per cell in the same cultures declined fourfold, with a similar rate as the previous increase. At the beginning of the stationary phase, polyP amounts in  $P_{(+)}$  cells were low but still detectable with  $0.15 \pm 0.01 \text{ pg } P_i \cdot \text{cell}^{-1}$  and remained stable until the

resupply with  $P_{(+)}$  cultivation medium at day 15 (ANOVA:  $F_{3,11} = 1.511$ ;  $p = 0.266$ ; Figure 5c). In  $P_{(-)}$  cells, cellular amounts of polyP were stable during the lag phase (Student test:  $t(6) = 2.995$ ,  $p = 0.058$ ), and immediately declined at a rate of  $0.13 \pm 0.02 \text{ pg } P_i \cdot \text{cell}^{-1} \cdot \text{day}^{-1}$  at the onset of cell division from day 2 to day 4. During the same period, polyP concentration was 42 times lower than in  $P_{(+)}$  cells but still detectable with  $0.04 \pm 0.01 \text{ pg } P_i \cdot \text{cell}^{-1}$  on day 4 (Figure 5c). Already at day 6, polyP was no longer detectable in  $P_{(-)}$  cells (Figure 5c).

After phosphate supplementation on day 15,  $P_{(+/+)}$  and  $P_{(-/+)}$  cultures responded differently. Within the 24 h lag phase,  $P_{(-/+)}$  cells generated three times more polyP with  $1.80 \pm 0.30 \text{ pg } P_i \cdot \text{cell}^{-1}$  compared to  $0.60 \pm 0.10 \text{ pg } P_i \cdot \text{cell}^{-1}$  in  $P_{(+/+)}$  cells (Figure 5c, Table S5 in the Supporting Information). This strong increase in polyP stocks in  $P_{(-/+)}$

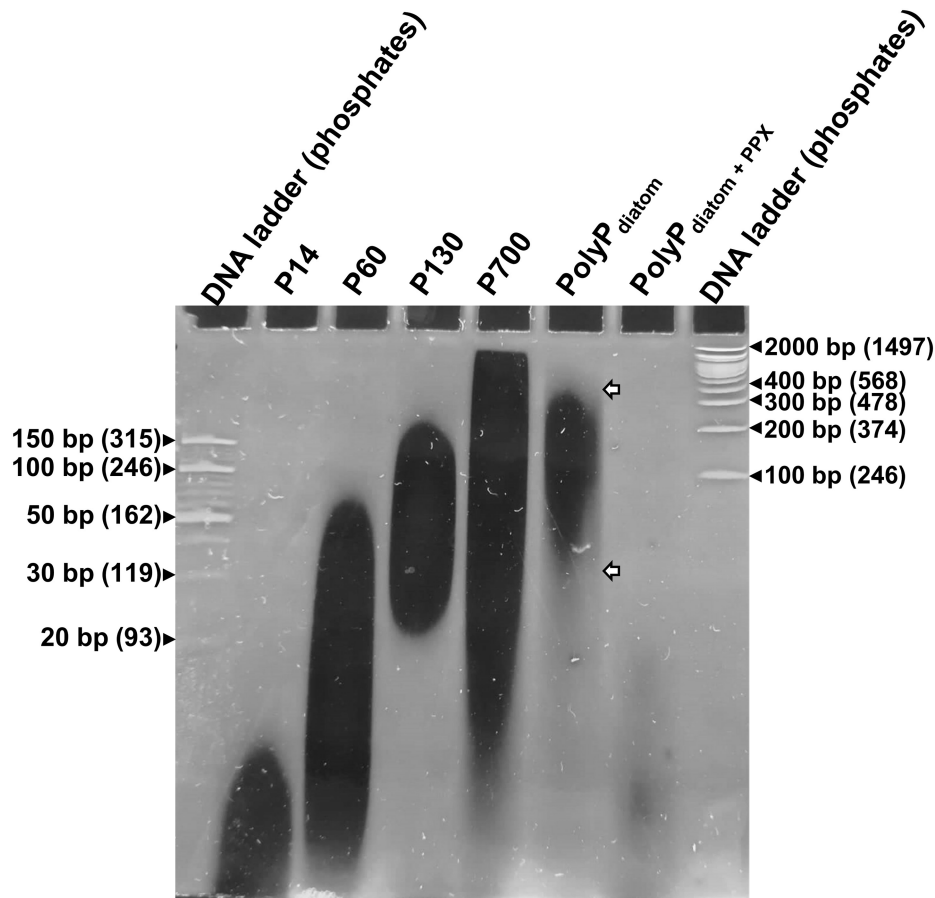


**FIGURE 4** Twenty percent TBE-urea gel electrophoresis of polyP extracted from *Achnantheidium minutissimum* cultivated in P-replete  $P_{(+)}$  conditions. PolyP is stained with DAPI. The lanes show (from left to right) a 10bp DNA marker, the polyP standards polyP-14, 60, 130, and 700  $P_i$ , polyP extracted from *A. minutissimum* (PolyP<sub>diatom</sub>), polyP extracted from the diatom and treated with exopolyphosphatase (PPX) (PolyP<sub>diatom+PPX</sub>), and a 100bp DNA marker (Invitrogen). Labels of DNA ladders indicate the size of the ladders in base pairs (bp) as well as their equivalent in  $P_i$  units (in brackets) for polyP length determination following the calculation of Smith et al. (2018). White arrows indicate the upper and lower limit of the polyP range extracted from the diatom.

cells measured 24 h after  $P_i$  resupply was accompanied by a faster exogenous  $P_i$  uptake per cell during the same period, taking up exogenous P threefold faster than  $P_{(+/+)}$  cells with an uptake rate of  $2.13 \pm 0.87 \text{ pg } P_i \cdot \text{cell}^{-1} \cdot \text{day}^{-1}$  compared with  $7.07 \pm 0.68 \text{ pg } P_i \cdot \text{cell}^{-1} \cdot \text{day}^{-1}$ , respectively (Figure 5d). Between days 2 and 4, ~20% of the P uptake was allocated to polyP production in  $P_{(+)}$  cells, and 24 h after phosphate supplementation, ~30% of the P uptake was allocated to polyP synthesis of  $P_{(-/+)}$  cells, against ~20% for  $P_{(+/+)}$  cells (Table S6 in the Supporting Information). The strong capability to take up extracellular  $P_i$  in  $P_{(-/+)}$  cells changed at the onset of cell division on day 17. During this period, the extracellular  $P_i$  uptake in  $P_{(-/+)}$  cells decreased fourfold, with an uptake rate of  $1.74 \pm 0.4 \text{ pg } P_i \cdot \text{cell}^{-1} \cdot \text{day}^{-1}$  and was 1.4 times lower than in  $P_{(+/+)}$  cells (Figure 5d). The amounts of polyP in  $P_{(-/+)}$  cells at day 17 remained high and were comparable to those observed before the start of cell division on day 16 (Student test:  $t(6) = 0.774$ ,  $p = 0.468$ ; Figure 5c). At day 18, cells were continuing to divide and the uptake rates of  $P_i$  in both  $P_{(+/+)}$  and  $P_{(-/+)}$  cells decreased to reach similar levels with  $0.58 \pm 0.11 \text{ pg } P_i \cdot \text{cell}^{-1} \cdot \text{day}^{-1}$  and  $0.69 \pm 0.13 \text{ pg}$

$P_i \cdot \text{cell}^{-1} \cdot \text{day}^{-1}$  (Student test:  $t(6) = 1.276$ ,  $p = 0.249$ ; Figure 5d). Extracellular  $P_i$  was depleted in both cultures on day 18 (Figure 5b). Similar to the observations for  $P_{(+)}$  cells at day 6,  $P_i$  starvation at day 18 was accompanied by a decrease of polyP amounts which was twofold higher in  $P_{(-/+)}$  than in  $P_{(+/+)}$  cells ( $1.3 \pm 0.2 \text{ pg } P_i \cdot \text{cell}^{-1} \cdot \text{day}^{-1}$  and  $0.7 \text{ pg } P_i \cdot \text{cell}^{-1} \cdot \text{day}^{-1}$ ; Figure 5d).

The Spearman's rank correlation coefficient matrix from the combined as well as separated  $P_{(+)}$  and  $P_{(-)}$  datasets revealed statistically significant strong positive relationships ( $R > 0.6$ ) among polyP concentration,  $P_i$  uptake, and external  $P_i$  concentration (Figure S3A–C in the Supporting Information). We also observed similar correlations when datasets were treated separately, with the strongest correlation seen between external  $P_i$  concentrations and the  $P_i$  uptake in  $P_{(-)}$  treatment (Figure S3A). There were no significant correlations between growth rate and polyP concentration,  $P_i$  uptake, or external  $P_i$  concentration in either the separated or the combined dataset (Figure S3A–C).

Using the same cultivation samples, polyP granules dynamics within the diatoms were followed by SRS



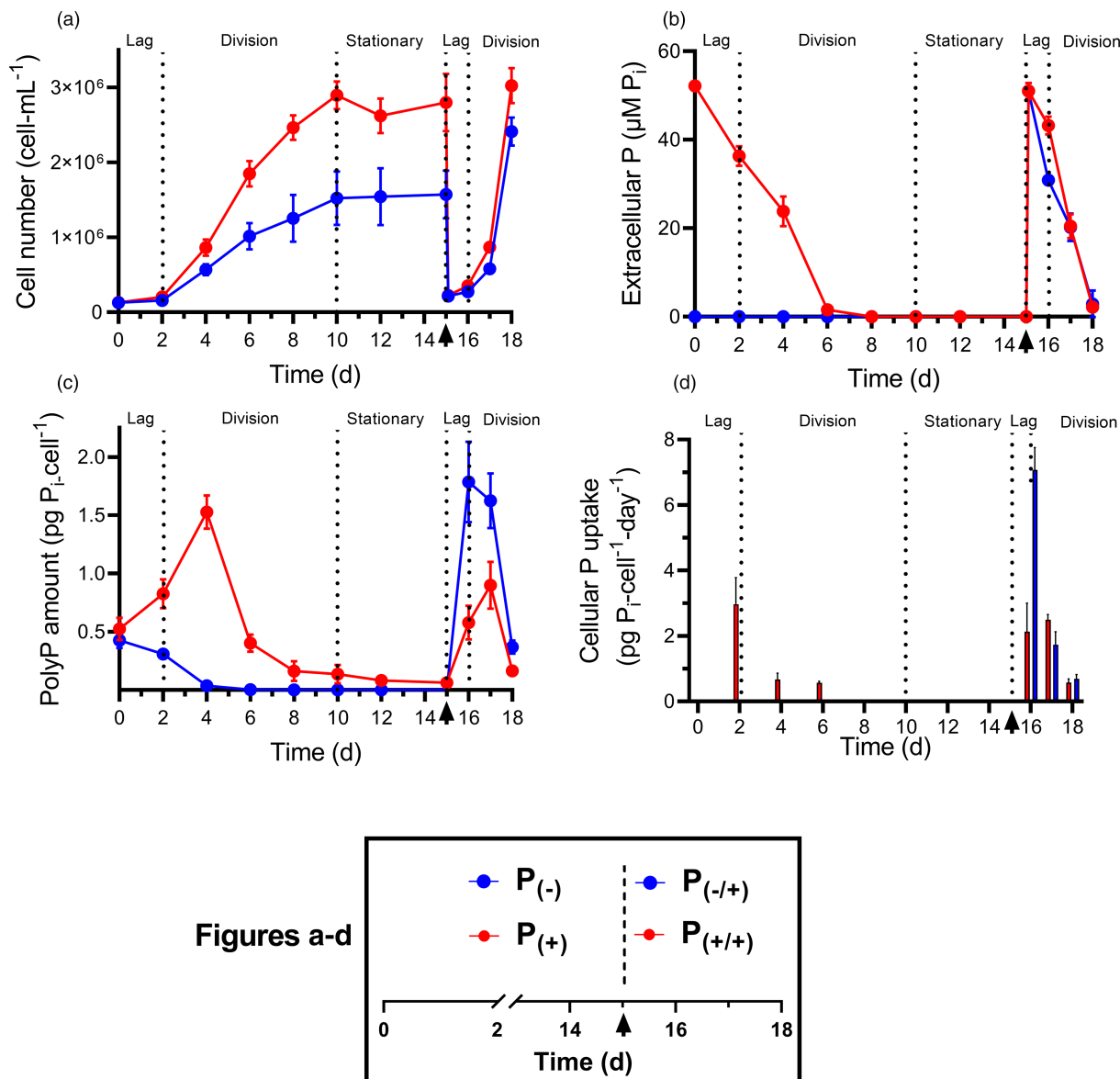


**FIGURE 5** Cultivation of *Achnanthydium minutissimum* under different P availabilities. Cells were cultivated for 15 days in either P-replete ( $P_{(+)}$ ) or P-deplete ( $P_{(-)}$ ) cultivation medium. Black arrows represent the time point of resupply with  $P_{(+)}$  cultivation medium in  $P_{(+)}$  and  $P_{(-)}$  cultures (day 15), and cells were annotated  $P_{(+/+)}$  and  $P_{(-/+)}$ , respectively.  $P_{(+/+)}$  and  $P_{(-/+)}$  cultures were incubated for 3 more days. (a) Cell growth ( $\text{cell}\cdot\text{mL}^{-1}$ ), (b) Dissolved extracellular P concentrations in the cultivation medium ( $\mu\text{M } P_i$ ), (c) Changes in cellular polyP content ( $\text{pg } P_i\cdot\text{cell}^{-1}$ ), (d) Changes in P uptake ( $\text{pg } P_i\cdot\text{cell}^{-1}\cdot\text{day}^{-1}$ ). Error bars indicate the standard deviation of  $n=4$  replicates. On day 15, data from (c) correspond to before the resupply in AM  $P_{(+)}$  cultivation medium, and (a) and (b) show data from before as well as after medium resupply with a difference of ca. 120 min between measurements. [Color figure can be viewed at [wileyonlinelibrary.com](https://onlinelibrary.wiley.com/terms-and-conditions)]

image analysis. The SRS data (Figure 6) confirm the quantitative polyP analyses as shown in Figure 5c. Granules were visible on day 0 in 50% of  $P_{(-)}$  cells and 53% of  $P_{(+)}$  cells (Figure S4A in the Supporting Information), and the percentage of surface area per cell occupied by the polyP granules was similar for both treatments at 6% (Figure S4B). On day 4, 79% of  $P_{(+)}$  cells were displaying polyP granules and only 9% of  $P_{(-)}$  cells, and granules were occupying a higher surface area in  $P_{(+)}$  cells at ~7.00% compared to 4.23% in  $P_{(-)}$  cells. On days 10 and 15, polyP granules were almost absent from  $P_{(-)}$  cells with only 4% and 3% of

cells containing granules, respectively. In contrast, in  $P_{(+)}$  cells, although polyP amounts were low when extracellular P concentrations were below the LOQ, 18% and 12% of cells were displaying visible granules on days 10 and 15, respectively (Figure 6). Only 24 h after phosphate resupply, polyP granules were present in 84% and 80% in both types of cells, respectively (Figures 5 and S4A). However, the percentage of surface area occupied by granules in cells was higher in  $P_{(-/+)}$  cells than in  $P_{(+/+)}$  cells with 8.33% compared to 5.36%, respectively (Figure S4B). At day 17, a majority of  $P_{(-/+)}$  and  $P_{(+/+)}$  cells still had granules, at 80%

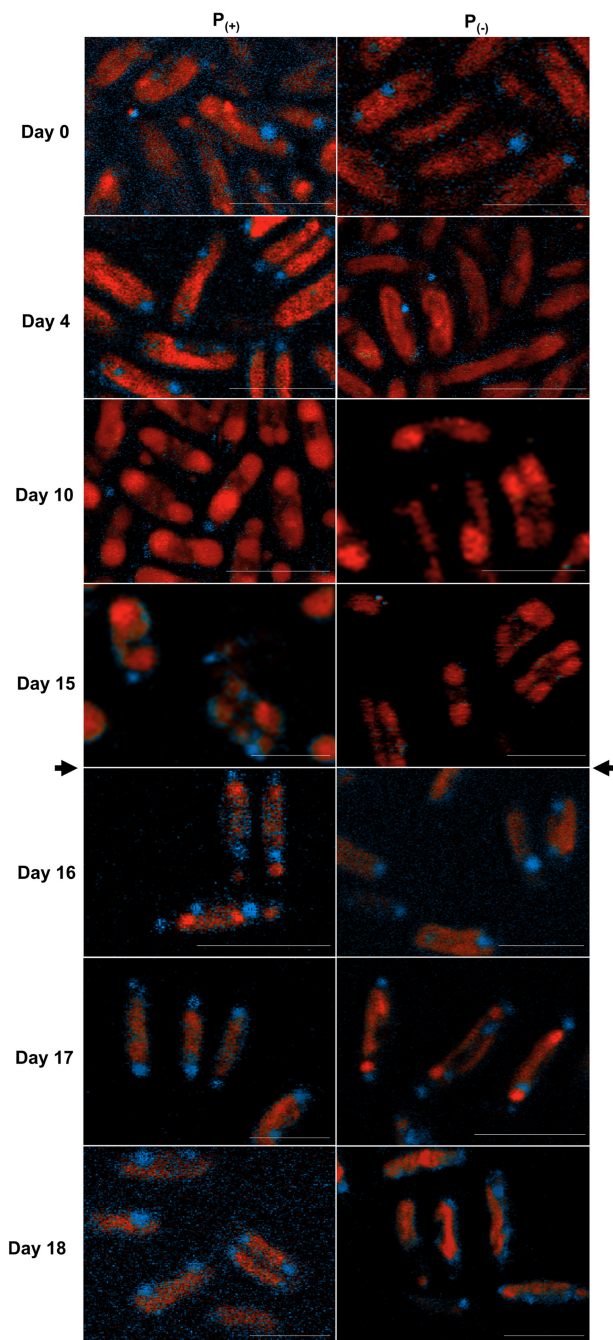


**FIGURE 6** SRS images of *Achnantheidium minutissimum* cells showing the dynamic of polyP granules (blue pixels) and lipids (red pixels) in cells before and after medium resupply. On day 15, data correspond to before the resupply in  $P_{(+)}$  cultivation medium. The scale bars correspond to 10  $\mu\text{m}$ . [Color figure can be viewed at [wileyonlinelibrary.com](http://wileyonlinelibrary.com)]

and 75%, respectively. At day 18, when extracellular P concentrations were below the LOQ but cells were still growing, the amount of cells displaying polyP granules decreased, to 44% and 34% for  $P_{(-/+)}$  and  $P_{(+/+)}$  cells, respectively (Figure S4A). Similarly, the percentage of surface area occupied by the granules also decreased to 5.19% and 4.68% in both  $P_{(-/+)}$  and  $P_{(+/+)}$  cells, respectively (Figure S4B).

## DISCUSSION

### *Achnantheidium minutissimum* stores polyP granules in vacuoles resembling acidocalcisomes organelles

Raman spectroscopy, EDX microscopy, and biochemical analysis revealed that in the diatom *Achnantheidium minutissimum*, polyP is stored in granular form, located within cell vacuoles. The localization of the polyP granules in *A. minutissimum* confirms classical observations in raphid pennate diatoms describing two large apical vacuoles containing spherical “volutin granules,” also known as polyP granules (Mann, 1985, p. 99). The vacuoles contain polyP-Ca-rich granules and share anatomical and chemical features with acidocalcisomes (Docampo et al., 2005). These acidic organelles are considered to be major storage compartments in microorganisms for phosphorus compounds (orthophosphate, pyrophosphate, polyP), as well as cations (calcium, magnesium, iron ions; Docampo et al., 2005). The green alga *Chlamydomonas reinhardtii* also possesses acidocalcisomes; these contain polyP and  $\text{Ca}^{2+}$  ions and are surrounded by a membrane containing a vacuolar proton-translocating inorganic pyrophosphatases (V-H+ -PPase) and a vacuolar proton ATPase (V-H+ -ATPase; VHA), which generates a low pH in the organellar lumen (Ruiz et al., 2001). It has recently been demonstrated that the *Thalassiosira pseudonana* VHA is localized in the membranes of chloroplasts (Yee et al., 2023) and in silica deposition vesicles (SDVs), as well as in vacuoles (Yee et al., 2020). In addition, the vacuolar transport chaperone complex (VTC1-4) is important for polyP synthesis within yeast vacuoles (Secco et al., 2012) and in *C. reinhardtii* (Plouviez et al., 2021). The diatom *Phaeodactylum tricornum* encodes for homologs of VTC (PtVTC 1–4), but only the PtVTC2 was located in the vacuolar membrane region (Schreiber et al., 2017), while the homologs PtVTC1, PtVTC3, and PtVTC4 showed no vacuolar localization (Dell’Aquila et al., 2020). Sequence analyses of cDNA extracts have indicated that *A. minutissimum* possesses homologs of VHA and V-H+ -PPase, as well as the four subunits of the VTC complex (Dow, 2019). However, the localization of the VTC subunits and these proton pumps in *A. minutissimum* is unknown, and further studies are required to analyze the composition of these apical vacuoles containing polyP granules.

### The resistance of *Achnantheidium minutissimum* and reduction of polyP reservoirs under phosphate-limiting conditions

Based on the results presented here, we propose a scenario of cell responses to varying P availabilities (Figure 7), described below.

Although the cell density in cultures under  $P_{(+)}$  and  $P_{(-)}$  conditions was different at the end of the exponential phase, cells cultivated in  $P_{(-)}$  conditions continued to divide for another 8 days in the absence of available exogenous P and were able to resume P uptake and growth very quickly once P became available. This reflects the capability of this diatom to survive under varying external P availability, suggesting the presence of a metabolic poise that allows growth maintenance under short-term external P starvation. Applying SRS microscopy and biochemical analyses, we observed that dividing *Achnantheidium minutissimum* in  $P_{(+)}$  conditions accumulated polyP when extracellular  $P_i$  concentrations declined. Microorganisms subjected to  $P_{(+)}$  conditions can accumulate  $P_i$  from the environment in excess of that required for growth and store it as a reserve by synthesizing polyP chains when the external concentration of P is becoming limited (Kuhl, 1974). Such a response is called “luxury uptake” (Eixler et al., 2006; Li & Dittrich, 2019) and is thought to be essential for microorganisms to survive periods of scarce P availability (Solovchenko et al., 2020). In addition, yeast lacking the vacuolar transporter chaperone gene (VTC4), which is responsible for the synthesis of polyP from ATP, have shown reduced growth when cultivated under  $P_{(-)}$  conditions, suggesting that polyP is involved in cell survival during P stress (Hothorn et al., 2009). With no exogenous P available, we observed cellular polyP stocks in both  $P_{(+)}$  and  $P_{(-)}$  conditions decreased quickly as the cells were dividing, suggesting that polyP stocks in *A. minutissimum* may be used to sustain anabolic processes such as DNA synthesis (Figure 7). Thus, the depletion of polyP stocks acquired in  $P_{(+)}$  conditions in *A. minutissimum* cells may contribute to the P requirements for sustaining cellular processes under  $P_{(-)}$  conditions.

After polyP stock depletion in  $P_{(-)}$  conditions, the cells continued dividing for 4 more days. When subjected to P stress, diatoms and microalgae can reduce their cellular P demand by remodeling membrane lipids (Figure 7). The response is associated with a reduction of membrane phospholipids (PL) in favor of other lipids like betaine and sulfur-containing lipids (Huang et al., 2019; Martin et al., 2014; Van Mooy et al., 2009). This process results in a decrease in the cellular P demands (Hunter et al., 2018; Martin et al., 2011), sparing ~17% of the total P cell demand in marine microalgae (Van Mooy et al., 2009). A minor membrane PL degradation has been detected during lipidome remodeling in *Thalassiosira pseudonana* under P limitation, and the released P could support cell growth for additional 3 days (Hunter et al., 2018). Although the role of lipid membrane remodeling in alleviating external P limitation in *Achnantheidium minutissimum* is still speculative and needs further analyses, it is reasonable to assume that the diatom

uses other P reservoirs after the depletion of its polyP stocks.

## PolyP production of starved cells after phosphate resupply: The overplus mechanism

Within the first 24 h following the resupply of cultures with  $P_i$ , *Achnantheidium minutissimum* cells that were initially supplemented with  $P_{(-)}$  medium ( $P_{(-/+)}$ ) showed a threefold faster extracellular P uptake rate than cells that were initially supplemented with  $P_{(+)}$  medium ( $P_{(+/+)}$ ; Figure 7). Such a phenomenon in other microalgae has been termed “overplus response” (e.g., Aitchison & Butt, 1973; Harold, 1964; Liss & Langen, 1962; Plouviez et al., 2021). A rapid P uptake by  $P_{(-/+)}$  proves that *A. minutissimum* can drastically increase its P assimilation rate. For the uptake of extracellular P through the plasma membrane and its transport to organelles,  $P_i$ -transporters are essential. Transcriptomic data analyses have revealed that in *Thalassiosira pseudonana* and *Phaeodactylum tricornutum*, the expression of  $P_i$  transporter genes increases when the cells experience P deficiency (Alipanah et al., 2018; Dyhrman et al., 2012; Yang et al., 2014). The rapid P uptake per cell in *A. minutissimum*  $P_{(-/+)}$  cells was accompanied by a dramatic increase in their polyP levels. This is also consistent with the observations of overplus responses in cyanobacteria (Li & Dittrich, 2019) and in *Chlamydomonas reinhardtii* (Plouviez et al., 2021). Overplus responses are likely to play an important role in P retention in cells experiencing temporally variable P supply (Rhee, 1973). The usage of the P stored after overplus response for growth continuation has been shown in stream periphyton communities (Rier et al., 2016) as well as in cyanobacteria (Falkner & Falkner, 2011). Similarly, in our study, it is reasonable to assume that *A. minutissimum* may also have used the P stored (e.g., polyP stock) during the overplus response for sustaining growth under external P limitation. Hence, we suggest that *A. minutissimum* can respond rapidly to environmental P fluctuations by adjusting its P-uptake and polyP reserve metabolism. A remaining question is why the  $P_i$  uptake in  $P_{(+/+)}$  cells remained low 24 h after the resupply with  $P_{(+)}$  cultivation medium, even though cells experienced phosphorus limitation and growth cessation beforehand. Since P uptake rates in microalgae are dependent on the cellular P concentration (Caceres et al., 2019; Rhee, 1973), it is likely that  $P_{(+/+)}$  cells still possessed P reserves other than polyP, which prevented the diatom overplus response. The further identification of these reserves as well as the investigation of their co-dynamics under P limitation would greatly improve the understanding of the diatom P homeostasis.

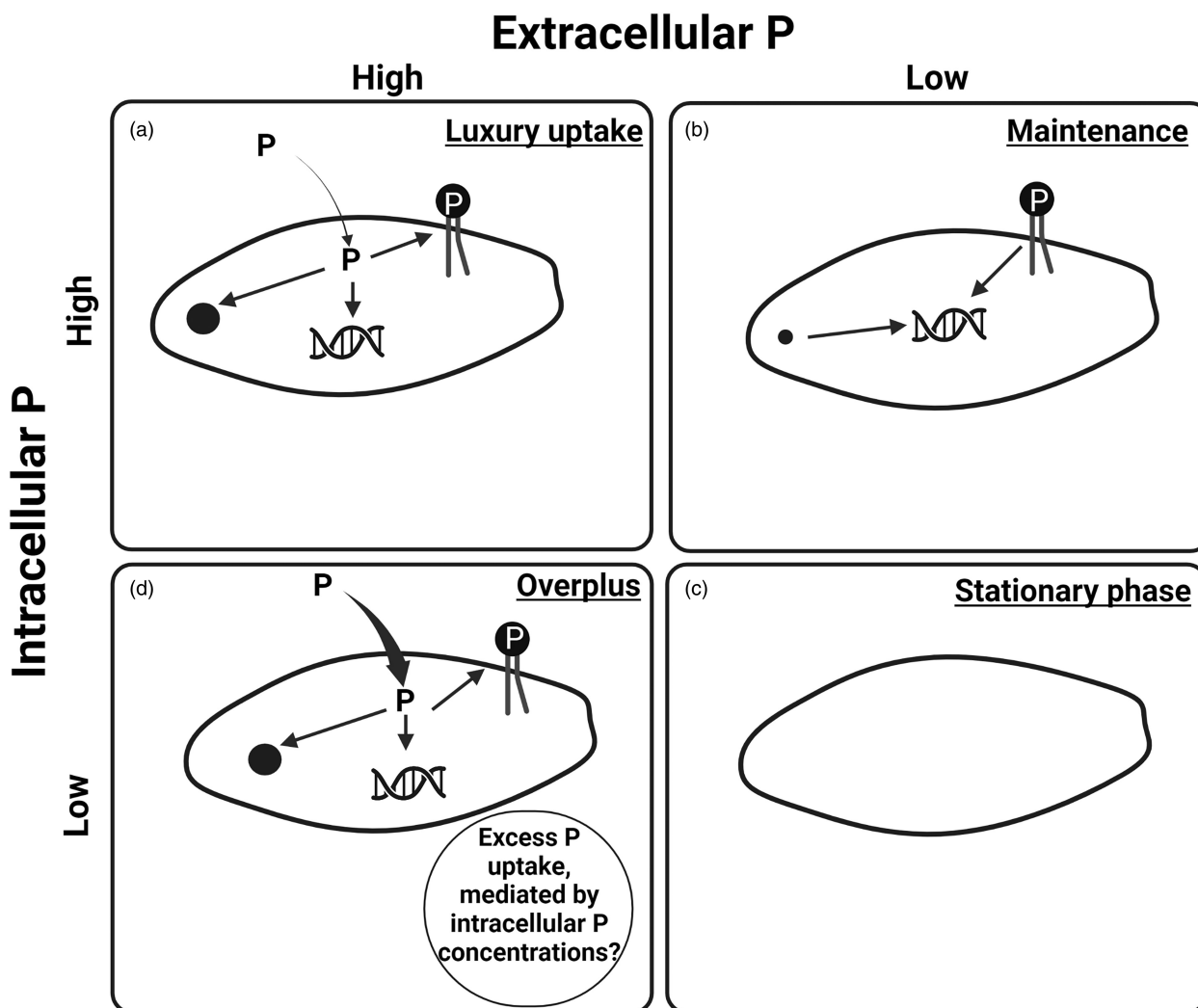


**FIGURE 7** Schematic figure showing the phosphorus (P) physiology of the diatom *Achnanthyidium minutissimum* in different nutrient availability scenarios, based on the data collected in this study. (a) In the presence of exogenous P, the diatom stored excess P not required for growth in polyP granules through the luxury uptake of P. (b) In the absence of exogenous P, the diatom used its polyP reserves to sustain its cellular P requirements, and growth was maintained. After the depletion of polyP reserves, further growth was sustained by other cellular P storages, e.g., phospholipids. (c) Growth of the diatom eventually halted when cellular P reserves were depleted. (d) Once the diatoms with low P reserves were resupplied with exogenous P, they took up large amounts of P and stored the P as polyP through the overplus response. Depending on the availability of external P, the diatom could either undergo a new low-P availability phase and use its P storages to maintain its growth or could transition to a luxury uptake phase where it stored excess P in polyP. Curved black arrows indicate the uptake of exogenous P. Straight black arrows indicate the phosphorus transfer processes. Black spheres indicate the polyphosphate (polyP) granules. The DNA symbol represents the diatom growth.

## CONCLUSIONS

The freshwater diatom *Achnanthyidium minutissimum* can accumulate polyP through the “luxury uptake” and “overplus response,” which are processes well documented in algae and other aquatic microorganisms but poorly understood in diatoms. These two strategies would provide a physiological advantage to the diatom in that it would be able to store P when it was available and later use it for growth when external P was depleted, for example in P-varying ecosystems. Further studies are needed to understand the relevance of polyP in diatoms. In this regard, SRS microscopy applications have a strong potential for fast detection of

polyP in diatom samples. In addition, studies need to be conducted to unravel the molecular pathways of polyP synthesis to better understand its regulation in diatoms.

## AUTHOR CONTRIBUTIONS

**Adrien Lapointe:** Conceptualization (lead); formal analysis (equal); investigation (lead); methodology (equal); project administration (lead); visualization (lead); writing – original draft (lead); writing – review and editing (equal). **Mustafa Kocademir:** Formal analysis (equal); investigation (equal); methodology (equal); visualization (equal); writing – review and editing (equal). **Paavo Bergmann:** Formal analysis (equal);

investigation (equal); methodology (equal); visualization (equal); writing – review and editing (equal). **Imaiyan Chitra Ragupathy:** Formal analysis (equal); investigation (equal); methodology (equal); software (equal); visualization (equal); writing – review and editing (equal). **Michael Laumann:** Formal analysis (equal); investigation (equal); methodology (equal); resources (equal); validation (equal); visualization (equal); writing – review and editing (equal). **Graham J. C. Underwood:** Formal analysis (equal); supervision (equal); writing – review and editing (equal). **Andreas Zumbusch:** Resources (equal); validation (equal). **Dieter Spittler:** Conceptualization (equal); supervision (equal); validation (equal); writing – review and editing (equal). **Peter G. Kroth:** Conceptualization (equal); funding acquisition (lead); resources (equal); supervision (equal); validation (equal); writing – review and editing (equal).

## ACKNOWLEDGMENTS

We are grateful for the financial support by the DFG (Deutsche Forschungsgemeinschaft)-GRK2272 (RTG R3). MK was supported by a Philipp–Schwartz stipend from the Alexander von Humboldt foundation. Part of this work received funding from the European Union's Horizon 2020 research and innovation program under grant agreement no. 812922. We thank RegeneTiss Incorporated (Tokyo, Japan) for the kind gift of the polyP standards. Open Access funding enabled and organized by Projekt DEAL.

## ORCID

Adrien Lapointe  <https://orcid.org/0000-0002-0382-6305>

Paavo Bergman  <https://orcid.org/0000-0002-4954-9294>

## REFERENCES

- Aitchison, P., & Butt, V. (1973). The relation between the synthesis of inorganic polyphosphate and phosphate uptake by *Chlorella vulgaris*. *Journal of Experimental Botany*, *24*, 497–510.
- Alipanah, L., Winge, P., Rohloff, J., Najafi, J., Brembu, T., & Bones, A. M. (2018). Molecular adaptations to phosphorus deprivation and comparison with nitrogen deprivation responses in the diatom *Phaeodactylum tricornutum*. *PLoS ONE*, *13*, e0193335.
- Armbrust, E. V. (2009). The life of diatoms in the world's oceans. *Nature*, *459*, 185–192.
- Babes, V. (1895). Beobachtungen über die metachromatischen Körperchen, Sporenbildung, Verzweigung, Kolben- und Kapselbildung pathogener Bakterien. *Zeitschrift für Hygiene und Infektionskrankheiten*, *20*(1), 412–437.
- Bedoshvili, Y., Gneusheva, K., Popova, M., Morozov, A., & Likhoshway, Y. (2018). Anomalies in the valve morphogenesis of the centric diatom alga *Aulacoseira islandica* caused by microtubule inhibitors. *Biology Open*, *7*(8), bio035519.
- Benitez-Nelson, C. R. (2000). The biogeochemical cycling of phosphorus in marine systems. *Earth Science Reviews*, *51*, 109–135.
- Bondoc, K. G. V., Lembke, C., Vyverman, W., & Pohnert, G. (2019). Selective chemoattraction of the benthic diatom *Seminavis robusa* to phosphate but not to inorganic nitrogen sources contributes to biofilm structuring. *Microbiology*, *8*, e00694.
- Brown, M. R., & Kornberg, A. (2004). Inorganic polyphosphate in the origin and survival of species. *Proceedings of the National Academy of Sciences of the United States of America*, *101*, 16085–16087.
- Bru, S., Samper-Martin, B., Quandt, E., Hernandez-Ortega, S., Martinez-Lainez, J. M., Gari, E., Rafel, M., Torres-Torronteras, J., Marti, R., Ribeiro, M. P. C., Jimenez, J., & Clotet, J. (2017). Polyphosphate is a key factor for cell survival after DNA damage in eukaryotic cells. *DNA Repair (Amst)*, *57*, 171–178.
- Caceres, C., Spatharis, S., Kaiserli, E., Smeti, E., Flowers, H., & Bonachela, J. A. (2019). Temporal phosphate gradients reveal diverse acclimation responses in phytoplankton phosphate uptake. *The ISME Journal*, *13*, 2834–2845.
- Cheng, J. X., & Xie, X. S. (2015). Vibrational spectroscopic imaging of living systems: An emerging platform for biology and medicine. *Science*, *350*(6264), aaa8870.
- Christ, J. J., & Blank, L. M. (2018). Enzymatic quantification and length determination of polyphosphate down to a chain length of two. *Analytical Biochemistry*, *548*, 82–90.
- De Jager, H. J., & Heyns, A. M. (1998). Study of the hydrolysis of sodium polyphosphate in water using Raman spectroscopy. *Applied Spectroscopy*, *52*(6), 808–814.
- Dell'Aquila, G., Zauner, S., Heimerl, T., Kahnt, J., Samel-Gondesen, V., Runge, S., Hempel, F., & Maier, U. G. (2020). Mobilization and cellular distribution of phosphate in the diatom *Phaeodactylum tricornutum*. *Frontiers in Plant Science*, *11*, 579.
- Diaz, J., Ingall, E., Benitez-Nelson, C., Paterson, D., de Jonge, M. D., McNulty, I., & Brandes, J. A. (2008). Marine polyphosphate: A key player in geologic phosphorus sequestration. *Science*, *320*, 652–655.
- Docampo, R., de Souza, W., Miranda, K., Rohloff, P., & Moreno, S. N. (2005). Acidocalcisomes – conserved from bacteria to man. *Nature Reviews. Microbiology*, *3*, 251–261.
- Dow, L. E. (2019). *Interactions between the freshwater benthic diatom Achnanidium minutissimum and the bacterium Dyadobacter sp. 32*. [Doctoral dissertation, University of Konstanz, Germany].
- Dyhrman, S. T., Jenkins, B. D., Rynearson, T. A., Saito, M. A., Mercier, M. L., Alexander, H., Whitney, L. P., Drzewianowski, A., Bulygin, V. V., Bertrand, E. M., Wu, Z., Benitez-Nelson, C., & Heithoff, A. (2012). The transcriptome and proteome of the diatom *Thalassiosira pseudonana* reveal a diverse phosphorus stress response. *PLoS ONE*, *7*, e33768.
- Eixler, S., Karsten, U., & Selig, U. (2006). Phosphorus storage in *Chlorella vulgaris* (Trebouxiophyceae, Chlorophyta) cells and its dependence on phosphate supply. *Phycologia*, *45*(1), 53–60.
- Falkner, G., & Falkner, R. (2011). The complex regulation of the phosphate uptake system of cyanobacteria. In G. Peschek, C. Obinger, & G. Renger (Eds.), *Bioenergetic processes of cyanobacteria* (pp. 109–130). Springer.
- Fernando, E. Y., McIlroy, S. J., Nierychlo, M., Herbst, F. A., Petriglieri, F., Schmid, M. C., Wagner, M., Nielsen, J. L., & Nielsen, P. H. (2019). Resolving the individual contribution of key microbial populations to enhanced biological phosphorus removal with Raman–FISH. *The ISME Journal*, *13*(8), 1933–1946.
- Fisher, K. A. (1971). Polyphosphate in a chlorococcalean alga. *Phycologia*, *10*, 177–182.
- Guillard, R. R. (1975). Culture of phytoplankton for feeding marine invertebrates. In W. L. Smith & M. H. Chanley (Eds.), *Culture of marine invertebrate animals: 1st conference on culture of marine invertebrate animal greenport* (pp. 29–60). Springer.
- Harold, F. (1964). Enzymic and genetic control of polyphosphate accumulation in *Aerobacter aerogenes*. *Microbiology*, *35*, 81–90.
- Hlubíková, D., Ector, L., & Hoffmann, L. (2011). Examination of the type material of some diatom species related to *Achnanidium minutissimum* (Kütz.) Czarn. (Bacillariophyceae). *Algalological Studies*, *136-137*, 19–43.

- Hothorn, M., Neumann, H., Lenherr, E. D., Wehner, M., Rybin, V., Hassa, P. O., Uttenweiler, A., Reinhardt, M., Schmidt, A., Seiler, J., Ladurner, A. G., Herrmann, C., Scheffzek, K., & Mayer, G. (2009). Catalytic core of a membrane-associated eukaryotic polyphosphate polymerase. *Science*, *324*, 513–516.
- Huang, B., Marchand, J., Blanckaert, V., Lukomska, E., Ulmann, L., Wielgosz-Collin, G., Rabesaotra, V., Moreau, B., Bougaran, G., Mimouni, V., & Morant-Manceau, A. (2019). Nitrogen and phosphorus limitations induce carbon partitioning and membrane lipid remodelling in the marine diatom *Phaeodactylum tricorutum*. *European Journal of Phycology*, *54*, 342–358.
- Huang, W., Rio Bartulos, C., & Kroth, P. G. (2016). Diatom vacuolar 1,6-beta-transglycosylases can functionally complement the respective yeast mutants. *The Journal of Eukaryotic Microbiology*, *63*, 536–546.
- Hunter, J. E., Brandsma, J., Dymond, M. K., Koster, G., Moore, C. M., Postle, A. D., Mills, R. A., & Attard, G. S. (2018). Lipidomics of *Thalassiosira pseudonana* under phosphorus stress reveal underlying phospholipid substitution dynamics and novel diglycosylceramide substitutes. *Applied and Environmental Microbiology*, *84*, e02034-17.
- Kuhl, A. (1974). Phosphorus. In W. D. P. Stewart (Ed.), *Algal physiology and biochemistry* (pp. 636–654). Blackwell Scientific.
- Lapointe, A., Spittler, D., & Kroth, P. G. (2022). High throughput method for extracting polyphosphates from diatoms. *Endocytosis and Cell Research*, *31*, 29–38.
- Leitão, J. M., Lorenz, B., Bachinski, N., Wilhelm, C., Müller, W. E., & Schröder, H. C. (1995). Osmotic-stress-induced synthesis and degradation of inorganic polyphosphates in the alga *Phaeodactylumtricorutum*. *Marine Ecology Progress Series*, *121*, 279–288.
- Levasseur, M., Thompson, P. A., & Harrison, P. J. (1993). Physiological acclimation of marine phytoplankton to different nitrogen sources. *Journal of Phycology*, *29*, 587–595.
- Li, J., & Dittrich, M. (2019). Dynamic polyphosphate metabolism in cyanobacteria responding to phosphorus availability. *Environmental Microbiology*, *21*, 572–583.
- Li, J., Plouchart, D., Zastepa, A., & Dittrich, M. (2019). Picoplankton accumulate and recycle polyphosphate to support high primary productivity in coastal Lake Ontario. *Scientific Reports*, *9*, 1–10.
- Lieberman, L. (1890). Detection of metaphosphoric acid in the nuclein of yeast. *Pflügers Archiv*, *47*, 155–160.
- Lin, S., Litaker, R. W., & Sunda, W. G. (2016). Phosphorus physiological ecology and molecular mechanisms in marine phytoplankton. *Journal of Phycology*, *52*, 10–36.
- Liss, E., & Langen, P. (1962). Experiments on polyphosphate overcompensation in yeast cells after phosphate deficiency. *Archiv für Mikrobiologie*, *41*, 383–392.
- Mann, D. (1985). In vivo observations of plastid and cell division in raphid diatoms and their relevance to diatom systematics. *Annals of Botany-London*, *55*, 95–108.
- Martin, P., Dyhrman, S. T., Lomas, M. W., Poulton, N. J., & Van Mooy, B. A. (2014). Accumulation and enhanced cycling of polyphosphate by Sargasso Sea plankton in response to low phosphorus. *Proceedings of the National Academy of Sciences of the United States of America*, *111*, 8089–8094.
- Martin, P., Van Mooy, B. A., Heithoff, A., & Dyhrman, S. T. (2011). Phosphorus supply drives rapid turnover of membrane phospholipids in the diatom *Thalassiosira pseudonana*. *The ISME Journal*, *5*, 1057–1060.
- Meyer, A. (1904). *Orientative studies on the distribution, morphology and chemistry of the volute*. A. Felix.
- Moudrikova, S., Sadowsky, A., Metzger, S., Nedbal, L., Mettler-Altmann, T., & Mojzes, P. (2017). Quantification of polyphosphate in microalgae by Raman microscopy and by a reference enzymatic assay. *Analytical Chemistry*, *89*, 12006–12013.
- Ogawa, N., DeRisi, J., & Brown, P. O. (2000). New components of a system for phosphate accumulation and polyphosphate metabolism in *Saccharomyces cerevisiae* revealed by genomic expression analysis. *Molecular Biology of the Cell*, *11*, 4309–4321.
- Paytan, A., & McLaughlin, K. (2007). The oceanic phosphorus cycle. *Chemical Reviews*, *107*, 563–576.
- Plouviez, M., Fernandez, E., Grossman, A. R., Sanz-Luque, E., Sells, M., Wheeler, D., & Guieysse, B. (2021). Responses of *Chlamydomonas reinhardtii* during the transition from P-deficient to P-sufficient growth (the P-overplus response): The roles of the vacuolar transport chaperones and polyphosphate synthesis. *Journal of Phycology*, *57*, 988–1003.
- Potapova, M., & Hamilton, P. B. (2007). Morphological and ecological variation within the *Achnanthyidium minutissimum* (Bacillariophyceae) species complex. *Journal of Phycology*, *43*, 561–575.
- Rao, N. N., Gomez-Garcia, M. R., & Kornberg, A. (2009). Inorganic polyphosphate: Essential for growth and survival. *Annual Review of Biochemistry*, *78*, 605–647.
- Rao, N. N., Liu, S., & Kornberg, A. (1998). Inorganic polyphosphate in *Escherichia coli*: The phosphate regulon and the stringent response. *Journal of Bacteriology*, *180*, 2186–2193.
- Rashid, M. H., Rumbaugh, K., Passador, L., Davies, D. G., Hamood, A. N., Iglewski, B. H., & Kornberg, A. (2000). Polyphosphate kinase is essential for biofilm development, quorum sensing, and virulence of *Pseudomonas aeruginosa*. *Proceedings of the National Academy of Sciences of the United States of America*, *97*, 9636–9641.
- Rhee, G. Y. (1973). A continuous culture study of phosphate uptake, growth rate and polyphosphate in *Scenedesmus* sp. *Journal of Phycology*, *9*, 495–506.
- Rier, S. T., Kinek, K. C., Hay, S. E., & Francoeur, S. N. (2016). Polyphosphate plays a vital role in the phosphorus dynamics of stream periphyton. *Freshwater Science*, *35*, 490–502.
- Round, F. E. (2004). pH scaling and diatom distribution. *Diatom*, *20*, 9–12.
- Ruiz, F. A., Marchesini, N., Seufferheld, M., Govindjee, & Docampo, R. (2001). The polyphosphate bodies of *Chlamydomonas reinhardtii* possess a proton-pumping pyrophosphatase and are similar to acidocalcisomes. *The Journal of Biological Chemistry*, *276*, 46196–46203.
- Sanz-Luque, E., Bhaya, D., & Grossman, A. R. (2020). Polyphosphate: A multifunctional metabolite in cyanobacteria and algae. *Frontiers in Plant Science*, *11*, 938.
- Schlösser, U. G. (1994). SAG-Sammlung von Algenkulturen at the University of Göttingen Catalogue of strains 1994. *Botanica Acta: Journal of the German Botanical Society*, *107*, 113–186.
- Schreiber, V., Dersch, J., Puzik, K., Bäcker, O., Liu, X., Stork, S., Schulz, J., Heimerl, T., Klingl, A., Zauner, S., & Maier, U. G. (2017). The central vacuole of the diatom *Phaeodactylum tricorutum*: Identification of new vacuolar membrane proteins and of a functional di-leucine-based targeting motif. *Protist*, *168*(3), 271–282.
- Secco, D., Wang, C., Shou, H., & Whelan, J. (2012). Phosphate homeostasis in the yeast *Saccharomyces cerevisiae*, the key role of the SPX domain-containing proteins. *FEBS Letters*, *586*(4), 289–295.
- Smith, S. A., & Morrissey, J. H. (2007). Sensitive fluorescence detection of polyphosphate in polyacrylamide gels using 4',6-diamidino-2-phenylindol. *Electrophoresis*, *28*, 3461–3465.
- Smith, S. A., Wang, Y., & Morrissey, J. H. (2018). DNA ladders can be used to size polyphosphate resolved by polyacrylamide gel electrophoresis. *Electrophoresis*, *39*, 2454–2459.
- Solovchenko, A., Gorelova, O., Karpova, O., Selyakh, I., Semenova, L., Chivkunova, O., Baulina, O., Vinogradova, E., Pugacheva, T., Scherbakov, P., Vasilieva, S., Lukyanov, A., & Lobakova, E. (2020). Phosphorus feast and famine in cyanobacteria: Is luxury uptake of the nutrient just a consequence of acclimation to its shortage? *Cell*, *9*, 1933.
- Trilisenko, L., Kulakovskaya, E., & Kulakovskaya, T. (2017). The cadmium tolerance in *Saccharomyces cerevisiae* depends on

- inorganic polyphosphate. *Journal of Basic Microbiology*, 57, 982–986.
- Van Mooy, B. A., Fredricks, H. F., Pedler, B. E., Dyhrman, S. T., Karl, D. M., Koblizek, M., Lomas, M. W., Mincer, T. J., Moore, L. R., Moutin, T., Rappe, M. S., & Webb, E. A. (2009). Phytoplankton in the ocean use non-phosphorus lipids in response to phosphorus scarcity. *Nature*, 458, 69–72.
- Wiame, J. M. (1947). Study of a polyphosphorus, basophilic and metachromatic substance in yeasts. *Biochimica et Biophysica Acta*, 1, 234–255.
- Windler, M. (2014). *Bacterial influence on diatoms from photoautotrophic freshwater biofilms*. [Doctoral dissertation, University of Konstanz, Germany].
- Windler, M., Gruber, A., & Kroth, P. G. (2012). Purification of benthic diatoms from associated bacteria using the antibiotic imipenem. *Endocytosis and Cell Research*, 22, 62–65.
- Xie, L., & Jakob, U. (2019). Inorganic polyphosphate, a multifunctional polyanionic protein scaffold. *Journal of Biological Chemistry*, 294(6), 2180–2190.
- Yang, Z. K., Zheng, J. W., Niu, Y. F., Yang, W. D., Liu, J. S., & Li, H. Y. (2014). Systems-level analysis of the metabolic responses of the diatom *Phaeodactylum tricornutum* to phosphorus stress. *Environmental Microbiology*, 16, 1793–1807.
- Yee, D. P., Hildebrand, M., & Tresguerres, M. (2020). Dynamic subcellular translocation of V-type H<sup>+</sup>-ATPase is essential for biomineralization of the diatom silica cell wall. *The New Phytologist*, 225(6), 2411–2422.
- Yee, D. P., Samo, T. J., Abbriano, R. M., Shimasaki, B., Vernet, M., Mayali, X., Weber, P. K., Mitchell, B. G., Hildebrand, M., Decelle, J., & Tresguerres, M. (2023). The V-type ATPase enhances photosynthesis in marine phytoplankton and further links phagocytosis to symbiogenesis. *Current Biology*, 33, 2541–2547.

## SUPPORTING INFORMATION

Additional supporting information can be found online in the Supporting Information section at the end of this article.

**Figure S1.** Ultrastructural SEM image of an *Achnanthes minutissimum* cell taken from the same sample containing the cell shown in Figure 1A. A) SEM picture of *A. minutissimum* containing a cytoplasmic bridge (CB), thylakoids (T), lipid droplets (LD), electron-dense granule (G), and (F) frustule. The area delimited by the white square in A) was subjected to energy-dispersive X-ray spectroscopy (EDX). EDX elemental mapping for B) calcium and C) phosphorous. These data are representative of cells cultivated in P-replete (P(+)) conditions. Scale bar: scanning electron micrograph: 1  $\mu\text{m}$ , elemental maps: 2.5  $\mu\text{m}$ .

**Figure S2.** *Achnanthes minutissimum* cells cultivated in P(+) condition. Diatom cells cultivated in P(+) conditions for 3 days (upper row) and 6 days (lower row). A) Bright-field micrographs. B) Chlorophyll fluorescence. C) BODIPY staining. D) Merged picture from B) and C).

**Figure S3.** Correlation matrices of cell growth rate, extracellular P, polyP amount and cellular P uptake in A) P(-) and P(+) combined datasets B) in P(-) dataset and C) in P(+) dataset. Correlations marked with an asterisk are significant (\*,  $p < 0.033$ ; \*\*,  $p < 0.02$ , \*\*\*,  $p < 0.001$ ).

**Figure S4.** Dynamics of the polyP granules in *Achnanthes minutissimum* in different P availabilities.

A) Percentage of cells containing at least one granule visible using SRS imaging, before and after resupply with AM P(+) cultivation medium. B) SRS data analysis of the dynamics of the area occupied by polyP granules per cell containing at least one granule, before and after resupply with AM P(+) cultivation medium. Black arrows represent the time point at day 15 of resupply with P(+) cultivation medium in P(+) and P(-) cultures, and cells were annotated P(+/+) and P(-/+), respectively. On day 15, data correspond to before the resupply in P(+) cultivation medium. Data represent  $n = 1$  replicate.

**Table S1.** Protocol for cell fixation and embedding for SEM visualization. “RT” is room temperature.

**Table S2.** Final cell densities of *Achnanthes minutissimum* (in cells  $\cdot \text{mL}^{-1}$ ) after 15 days of cultivation together with the growth rates ( $\mu$ ,  $\text{d}^{-1}$ ) during the exponential growth phase under P(+) and P(-) conditions before medium resupply. Data represent means and standard deviations of  $n = 4$  replicates. Values in the same column with different superscript letters present significant statistical differences ( $p < 0.05$ ).

**Table S3.** Final cell densities of *Achnanthes minutissimum* (cell  $\cdot \text{mL}^{-1}$ ) after 18 days of cultivation, and growth rates ( $\mu$ ,  $\text{d}^{-1}$ ) at exponential phase under P(+/+) or P(-/+) conditions after resupplying with AM P(+) medium at day 15. Data represent means and standard deviations of  $n = 4$  replicates. Values in the same column with different superscript letters indicate significant statistical differences ( $p < 0.05$ ).

**Table S4.** Rate of polyP synthesis and degradation ( $\text{pg Pi} \cdot \text{cell}^{-1} \cdot \text{day}^{-1}$ ), before media resupply for P(+) cultures, and after medium resupply at day 15 for P(+/+) cultures. (N/A) means that there are no data because polyP is not detectable.

**Table S5.** Rate of polyP synthesis and degradation ( $\text{pg Pi} \cdot \text{cell}^{-1} \cdot \text{day}^{-1}$ ), before media resupply for P(-) cultures, and after medium resupply at d 15 for P(-/+) cultures. (N/A) means that there are no data because polyP is not detectable.

**Table S6.** Exogenous Pi uptake allocated to polyP synthesis (%), before media resupply for P(+) and P(-) cells, and after medium resupply at day 15 for P(+/+) and P(-/+) cells. (N/A) means that there are no data because there is no polyP synthesis.

**How to cite this article:** Lapointe, A., Kocademir, M., Bergman, P., Ragupathy, I. C., Laumann, M., Underwood, G. J. C., Zumbusch, A., Spittler, D., & Kroth, P. G. (2024). Characterization of polyphosphate dynamics in the widespread freshwater diatom *Achnanthes minutissimum* under varying phosphorus supplies. *Journal of Phycology*, 60, 624–638. <https://doi.org/10.1111/jpy.13423>